Characterization of Freestanding Polymer Films for Application in 351-nm, High-Peak-Power Laser Systems

A major roadblock to rapid progress in laser fusion is the enormous price of the necessary experimental facilities. Currently under planning or nearing construction are 40-cm-clear-aperture (per beam line), 200-or-more-channel, glass-laser systems that will each cost in excess of U.S. $\$10^9$ in pursuit of laser-fusion research.[1] A sizable portion of this price bears witness to the costs of optical materials and of the precision manufacturing methods for treating these materials at aperture scales that, up to now, were the domain of astronomers. There is strong incentive for developing lower-cost, high-throughput manufacturing technology and materials engineering, yielding devices that meet all the performance challenges typically demanded by such lasers.

One key constraint to limiting laser-system cost by aperture downscaling is the so-called *laser-damage threshold*.[2] The higher the damage threshold for given system-operating conditions (wavelength, pulse length, etc.), the more photons per cm^2 and seconds may be passed through a given device without incurring permanent performance penalties. In the asymptotic limit of an infinite laser-damage threshold, one could build infinitely powerful lasers having very affordable, small apertures. Short of this elusive condition, however, the quest for higher thresholds is both a material-design and device-processing imperative. It must be kept in mind, though, that any enhanced laser-damage threshold is useful only if no other optical performance parameters are sacrificed in the process.

Among such parameters are *wavefront quality*, absence of, or at least control of, *birefringence*, and long-term environmental and photolytic stability of the material. The latter assuages the need for reworking, replacing, or swapping devices frequently and thus affects the *operating* costs of large-clear-aperture lasers. The former two parameters are essential to transporting beams both with minimum static phase-front error and without polarization error. Both are pivotal to efficient higher-harmonic frequency conversion and to good focusability of beams onto the fusion targets.

With these demands in mind, we recently set out to test the utility of thin polymer membranes (pellicles) in high-peak-power, UV lasers. Scale-up of such membranes, and their preparation under ultraclean conditions, has been spurred by advances in UV lithography[3] of both semiconductor wafers and liquid crystal displays. The specific aim in these applications is to prevent particulate from falling onto, or settling on, the lithographic photomasks. As these primary applications call for excellent material homogeneity and low UV-absorption loss in pellicles, key prerequisites for successful pellicle use on high-peak-power UV lasers seemed already met. In this article, we will present an account of initial tests of such pellicles under 351-nm irradiation conditions significantly higher in fluence than in normal, photolithographic use.

In the following sections, the foil materials will be defined, the test procedures explained, and test results presented.

Sample Characterization

During this screening samples from three vendors[4] were sorted according to whether or not they were offered for *i*-line lithography, i.e., transmittance tuned for a maximum at 365 nm and prepared from a polymer with 280-nm cutoff (cellulose derivative), or for 248-nm, deep-UV lithography. In the following, we will sidestep reporting on cellulose derivatives since these foils are, in the current context, not noteworthy. They do find use, however, in optical-fuse (i.e., “must fail”), power-limiting applications where defined or downward-adjustable laser-damage thresholds are a key performance requirement.

Vendors offer two pellicle options: bare, single-layer foils or multilayer combinations with antireflective properties. In either implementation, pellicles are thin enough to act as both optically self-referencing etalons and freestanding samples in Fourier-transform IR spectroscopy. As will be shown here, the latter method is a simple and effective analysis tool for specifying the chemical similarities and differences in the samples from various vendors.

For these tests, vendors were not required to supply samples of a *prescribed thickness*, but only of a thickness *typically supplied for lithography applications*. Data, including those in Fig. 73.42, are therefore results from slightly different-thickness films (between 0.9 μm and 2.9 μm).

Figure 73.42 shows an overlay of three samples' IR absorption over the 4000 cm^{-1} to 400 cm^{-1} spectral range. From the general features it becomes immediately apparent that there is prominent overlap among the samples, i.e., largely similar addition polymers are used by the various suppliers. All samples show a weak "waviness" in their spectra—a manifestation of the samples' etalon effect in this wavelength range. Note the absence of any signal in the 2800-cm^{-1} area, the characteristic band for alkyl signatures, as well as the absence of signal around 3200 cm^{-1} for alkenes. There are, instead, strong, overlapping peaks between 1200 and 1400 cm^{-1}, characteristic for condensed system carbon–fluorine *Q* vibrations.[5] This permits identification of the materials as highly fluorinated (*perfluorinated*) homo- or copolymers. A widely known example of such a compound is tetrafluoroethylene.

After expanding the "fingerprint region" (see Fig. 73.43), subtle differences between samples become noticeable. Transmittance dips at 1030 cm^{-1} and 980 cm^{-1} in sample 2 (throughout this article, samples will be simply identified with numerals 1, 2, and 3 corresponding to sources in Ref. 4) and absent in sample 1 can be assigned to CF_2–CO vibrations found in perfluorinated 1,3-dioxolanes.[6] This sample thus belongs to the group of copolymers of perfluorinated dioxolane and tetrafluoroethylene. For certain weight ratios between the two members,[7] this copolymer remains amorphous over a wide temperature range and becomes solvent-processable—an important advantage for manufacturing low-scatter-loss, low-birefringence optical films.

It must be mentioned here that fluoropolymers are not the only deep-UV lithography materials. As early as 1985, a U.S. patent granted to Duly *et al.*[8] disclosed a polymethylmethacrylate pellicle for deep-UV lithography. We did not prepare

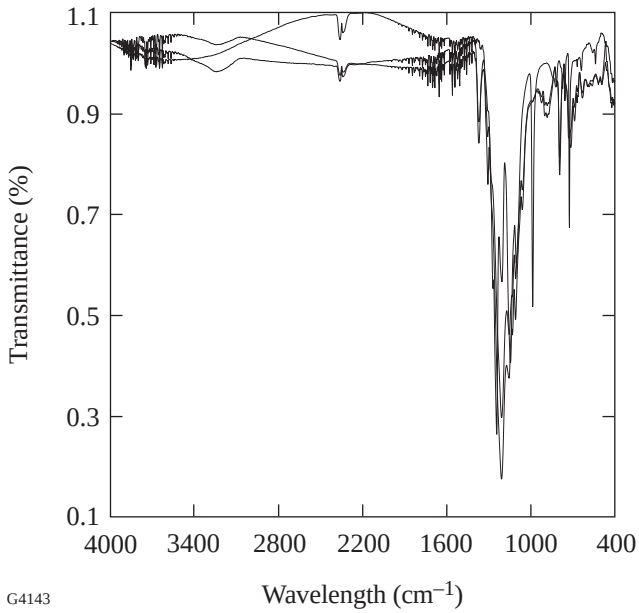

Figure 73.42
Infrared transmittance spectra (400 cm^{-1} to 4000 cm^{-1}) of the three sample types used in these measurements show the absence of alkyl and alkene characteristics (2900 cm^{-1} to 3200 cm^{-1}), while displaying strong carbon–fluorine vibrations.

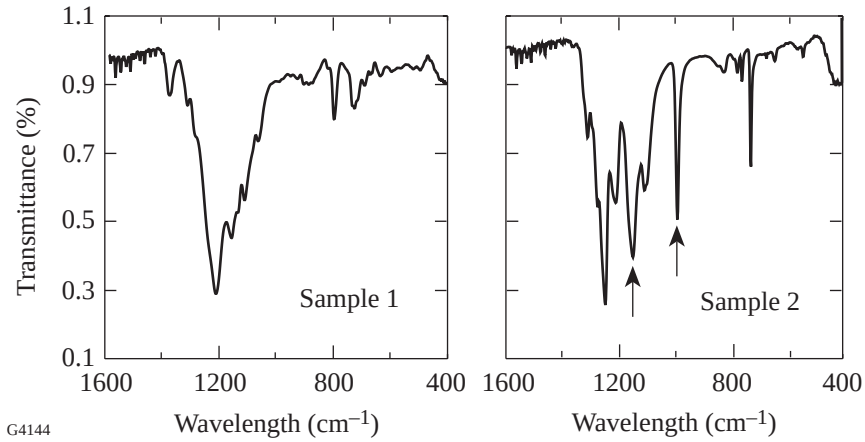

Figure 73.43
The "fingerprint" region (400 cm^{-1} to 1900 cm^{-1}) of the spectrum in Fig. 73.42. The fluorodioxolane signatures at 1030 cm^{-1} and 980 cm^{-1} are absent in sample 1 and highlighted in sample 2.

or obtain a pellicle from this material for comparison purposes; however, the issue of acrylates in high-peak-power laser use will be revisited during the discussion of current results.

Test Procedures

1. Damage-Threshold Measurements

A 7-s-repetition-rate, frequency-tripled Nd:glass laser in a standard laboratory environment is used for laser-damage testing. Its pulse length is 0.5 ns at the third harmonic, produced by Fourier-transform spectral narrowing through intracavity etalons, and the UV interaction spot size at the pellicle surface is 600 μm, produced by a 2-m-focal-length, fused-silica lens. The pulse length is sporadically monitored by a combination of a vacuum photodiode[9] and a 6-Ghz oscilloscope.[10] Each sample site is imaged under 110× dark-field microscopy both before and after laser irradiation. Any permanent, observable sample change is identified as damage.

At each irradiation instance, a digital record of the fluence distribution in a sample-equivalent plane is used to calculate the maximum shot fluence on target. Two irradiation modes are practiced: 1-on-1 and *N*-on-1. Samples are first tested in 1-on-1 mode and subsequently in *N*-on-1 mode. Mounted on a raster stage, random sample sites are moved into the irradiation position and irradiated by either one exposure (1-on-1 mode) or a sequence of increasingly intense pulses (*N*-on-1). The purpose of 1-on-1 irradiation lies in finding an *average damage threshold* averaged over a statistical number of sample sites. Backing off from this single-exposure average value by about a factor of 2, one may in subsequent *N*-on-1 testing start a fluence sequence at each *N*-on-1 site that ramps up until the damage fluence for each specific site has been found. Again this is carried out over a statistical number of sites. *N*-on-1 testing offers the more *realistic* threshold values as it simulates multishot, in-system-use conditions and accounts for various material-hardening effects known from the literature.[11]

In the case of 1-on-1 measurements, the average threshold value is the mean between the *highest nondamaging fluence* and the *lowest damaging fluence*, with the error derived from summing over all data points within the interval bracketed by these two fluences.

2. Photolysis Characterization

Long-term photolytic stability, i.e., change in sample absorbance in response to a large number of irradiations (1000) by *below-average-damage-threshold fluences* (nominally 3 J/cm^2, i.e., the maximum 351-nm system-design fluence on the OMEGA laser), is monitored by a calorimeter pair that samples the ratio of incident to transmitted pulse energy. To save time, a 5-s pulse repetition period is chosen. As a consequence, the unequal decay times of the two calorimeters introduce a constant bias that is measured under "sample absent" conditions over several hundred shots. Its slope is subsequently compared with that obtained under "sample in" conditions. Any observable *slope* differences are manifestations of sample photolysis effects.

This qualitative procedure is preferred over spectrophotometric measurements that offer quantitative results because of the small irradiation spot size (see previous section) and the associated registration accuracies involved in moving samples from one instrument to another. Even after registration issues are resolved, the task becomes one of microspectrophotometry, i.e, special effort has to be made to probe only the prior irradiated sample area if measurement sensitivity is to be kept acceptable.

3. Birefringence

Sample birefringence was evaluated by two methods: (1) a facile, low-contrast, visual check across the entire aperture between crossed sheet polarizers (100:1 contrast), and (2) a spot-by-spot measurement using a laser ellipsometer at 1053 nm. In this instrument, the sensitivity limit is 1/40 of a wave retardance averaged across a 0.8-mm spot size.

4. Interferometry in Transmission

A commercial interferometer[12] at $\lambda = 633$ nm was used to measure *transmission* wavefront errors in a double-pass mode. The interferometer is housed in a vibration-isolated, temperature- and air-draft–controlled enclosure.

Results

Even a decade ago, serious attempts at strengthening the laser-damage threshold of polymers[13] pointed out the critical importance of removing trace impurities from the (polyacrylic) polymer matrix. With the absorbance criterion having been made more rigorous since then by lithography demands, materials and processes for pellicles in 248-nm KrF excimer-laser lithography undergo strict optical-loss control,[3] both in terms of particulate as well as dissolved absorbers. It is thus not fully unexpected that we are able to report here the highest, 351-nm-laser-damage thresholds in our records covering tests on inorganic and organic optical materials for more than 15 years. The results are summarized in Fig. 73.44.

In Fig. 73.44, 1-on-1 and *N*-on-1 thresholds for the three vendors' foils are displayed. Although there is considerable variation among the thresholds for pellicles from different vendors, even the lowest reported threshold among them at 20 J/cm^2 is well above any operational 351-nm fluence on any large-scale glass laser in use or under design to date. Regarding these values, an important distinction must be made. In the **Test Procedures** section, the methodology for arriving at damage-threshold values was described. The thresholds marked with an asterisk in Fig. 73.44, i.e., those above 42 J/cm^2, *do not strictly comply* with this methodology for the following reason: The laser in use is *unable to generate the fluences at the given interaction spot size*, necessary to ascertain the *highest nondamaging fluence*. Thresholds marked with an asterisk represent the lowest damaging fluence obtainable from our laser at this spot size *for this given material*. In this regard, the perfluorinated pellicles are unique among the 1780 samples damage tested at this facility to date. They may also be unique at still shorter wavelengths.[14]

An additional challenge in determining these extraordinarily high thresholds derives from the interaction of the laser beam with air: at the stated fluences, particulates in air may get ionized near the sample surface and, pellicles being excellent dielectrics, locally charge the polymer. It becomes a daunting task to distinguish the electrostatically adhering particulates from "genuine damage" scatter sites. The threshold for vendor 3 at 69 J/cm^2 is an average over two sites on two films, both sites exhibiting a single detectable scatterer that remains uncertain as to whether or not it attracted dust.

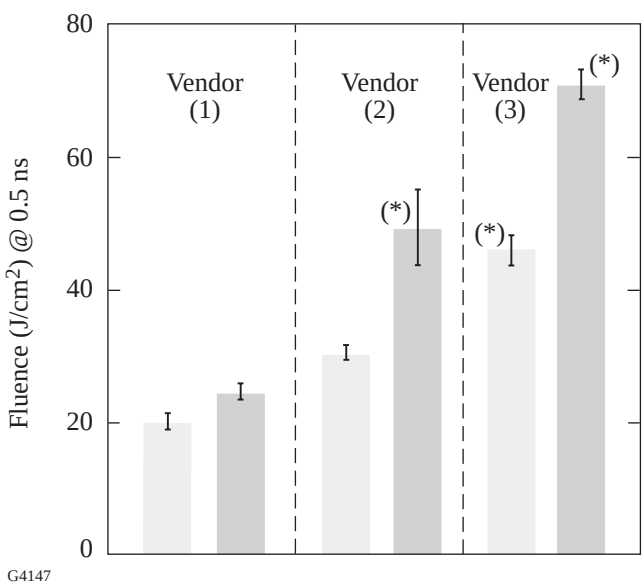

Figure 73.44
1-on-1 (light gray) and *N*-on-1 (dark gray) average damage thresholds for the three sample types identified as (1), (2), and (3) and tested at 351 nm (0.5-ns pulse length). Different sample types were received from different vendors. For the meaning of the asterisks, consult the text.

Figure 73.44 also reveals a consistent hardening in all samples upon multiple irradiation, i.e., the *N*-on-1 thresholds exceed the 1-on-1 thresholds by up to 30%. While this effect is neither new nor unique to these samples, it must be noted that the just-mentioned charging by air ionization may provide the basis for photorefractive effects in these polymers. In this instance, charge-separation time constants are critical, and the damage thresholds measured at the very-low repetition governing the current *N*-on-1 measurements, i.e., the sample is investigated after *each* exposure, are expected to be different from those that one would obtain under *high-repetition-rate* conditions. Such tests are still to be carried out.

For comparison, 351-nm bulk damage fluences for KDP (potassium dihydrogen phosphate) frequency-conversion crystals, as acquired for the OMEGA laser during the last five years, are lower by factors of 3 to 5 (with current crystal-growth technology, the canonical number is 10 J/cm^2 @ 351 nm, 1 ns). Three factors seem responsible for this remarkable superiority in damage-threshold values: (1) There is the already-mentioned attention to purity in starting materials and cleanliness in membrane processing. (2) More importantly, these pellicles intrinsically do not have to suffer the violent intrusions by grinding and polishing, typical for conventional optical elements, in order to achieve the transmission-wavefront uniformity reported below. (3) Being freestanding, frame-supported films, they expose very little bulk to the transiting laser pulse. Since thermodynamics requires that a finite density of defects must exist, even in very pure materials, this last property may be the pellicles' greatest asset in laser applications.

These advantages are further illustrated by data in Table 73.V, where 351-nm damage-threshold values are listed for a 240-nm-thick, inorganic, SiO_x film simultaneously vacuum-deposited on three different substrates and damage tested concurrently with the pellicles, i.e., under similar irradiation conditions. (The film stoichiometry is identified with only *x* here since no effort was made to accurately ascertain its value. We believe that $x = 2$.) This comparison shows how severe a price is paid for grinding and polishing: the damage threshold for the same film drops by an order of magnitude, depending on whether it is deposited on a conventionally

Table 73.V: Comparison of 351-nm, 0.5-ns laser-damage thresholds in J/cm^2 for a 240-nm-thick SiO_2 film concurrently vacuum deposited on three select surfaces: conventionally polished and cleaned fused silica,[15] freshly cleaved fused silica,[15] and freshly cleaved float glass.

Substrate Material and Surface Condition	Damage threshold (J/cm^2)	
	1-on-1	N-on-1
Polished fused silica	6.9±0.3	9.7±1.1
Cleaved fused silica	22.8±2.5	34.6±2.0
Cleaved float glass	27.7±1.3	24.5±2.0

prepared and cleaned fused silica[15] surface or on a freshly cleaved, otherwise untreated surface of either fused silica or inexpensive float glass. A lift-off technology, as is applied to the preparation of pellicles, can avoid this downside of conventional manufacturing.

As the sample films are homogenous, single-material layers, the *E*-field distributions of the transiting laser pulse inside the polymer are expected to *not exceed* the corresponding magnitudes *in vacuo*. No *E*-field *enhancement* needs to be considered in determining laser-damage thresholds for these films.

Next, we address sample *birefringence* results. Figure 73.45 shows a side-by-side comparison of parallel polarizers and crossed polarizers. Also included in the images is an extruded, 5-μm-thick Mylar® foil[16] whose intrinsic birefringence pattern in the two cases offers an instructive reference. Similar data exist, but are not shown here, for all vendors' pellicles. In quantitative terms (ellipsometry), no pellicle, including those with clear apertures as large as 30 cm, offered a single site in which the local birefringence exceeded the instrument sensitivity (λ/40 @ 1053 nm). Moreover, by applying uniaxial stress to square-frame–mounted pellicles of 0.9-mm thickness, even at stresses that visibly (unaided eye) distorted the frame, induced film birefringence remained below instrument sensitivity. In accordance with vendor specifications,[17] the stress-optic coefficient for perfluorinated-pellicle materials lies within 10% of that of the widely used stress-modeling material polymethacrylate. Owing to their short pathlength, however, pellicle films, even if nonuniformly stressed by, for instance, mounting or temperature biases, respond with retardance excursions tolerable in most high-peak-power laser systems.

Long-term photolytic stability, as measured by energy ratiometry, shows no measurable increase in absorptance in perfluorinated foils after 1000 exposures at nominally 3-J/cm^2 fluences per given site. The data shown in Fig. 73.46 represent ten-shot average values per data point for two cases: solid circles are data for beams passed through samples; open circles for "no-sample" conditions. The horizontal axis marks a cumulative number of shots. The offset between the two similarly sloped curves corresponds to the Fresnel insertion loss for this particular sample (16%, includes etalon reflectance and absorption). The slope itself is a result of unequal amounts of energy being deposited in each calorimeter at a repetition rate shorter than the thermal decay time of the calorimeter(s). Since any long-term increase (or decrease) in sample absorbance would have to manifest itself in a *change* in this slope,

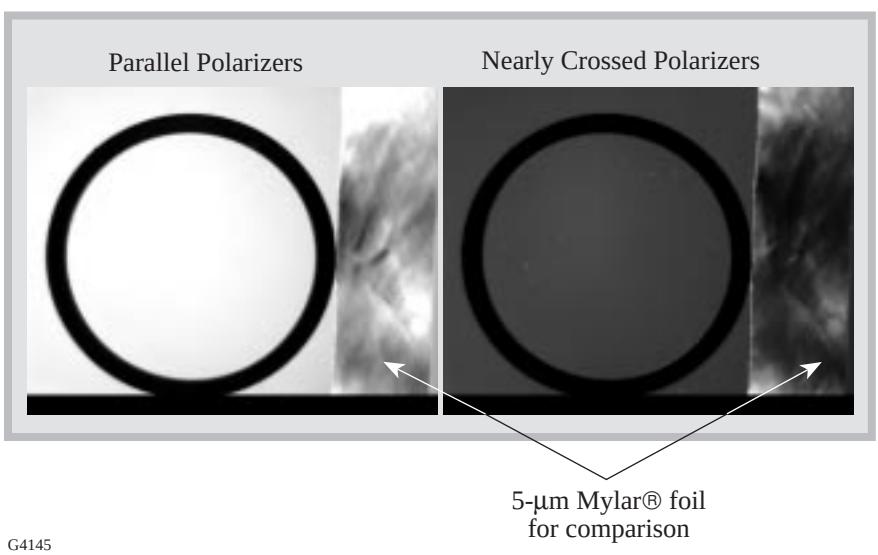

G4145

Figure 73.45
Comparison of birefringence between a 5-cm-clear-aperture, perfluorinated pellicle and an extruded, 5-μm-thick Mylar® foil placed between (a) parallel and (b) nearly crossed polarizers. Note the extensive stress birefringence imparted onto the Mylar® foil by the manufacturing process.

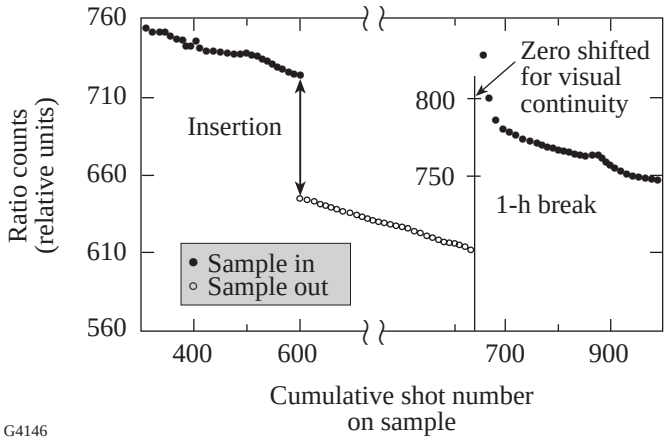

Figure 73.46
Calorimetric ratios of incident over transmitted energy (each data point is a ten-shot average) as a function of accumulated exposure. Nominal fluences on each shot were 3 J/cm^2. Full circles: sample in the beam; open circles: sample out.

the good agreement among slopes in Fig. 73.46 is taken as evidence for sufficient absence of such a cumulative absorbance increase. For a much smaller number of exposures per site, this is further corroborated by the distinction between 1-on-1 and *N*-on-1 thresholds depicted in Fig. 73.44. If there was substantial photolytic activity present in these samples, the evidenced "hardening" trend among all three sample types would be reversed.

We note here in passing that this absence of photolytic processes distinguishes the perfluorinated foils from cellulose-derivative ones, which, owing to such "photorefractive" response, give rise to interesting nonlinear scattering phenomena.[18] We note further that future large-scale laser systems are designed for >3-J/cm^2 maximum 351-nm fluence. Long-term photolytic stability in the 10- to 20-J/cm^2 fluence range still remains to be tested.

We also note that within the limited laser-output-power/spot-size phase space of our setup, i.e., a limited-range intensity gainlength test, a special effort to detect transverse stimulated Brillouin scattering yielded only *null results* in perfluorinated samples.

Interferometric tests of *thickness uniformity* (wavefront uniformity) pose a genuine challenge: the phase error measured between two consecutive, *empty-cavity* scans taken 10 min apart *is larger than* the phase error detectable *after the pellicle is inserted*. This result is true for pellicles up to 40 cm long (longest dimension). Thus, pellicle uniformity is better than can be measured with current state-of-the-art interferometers. This was independently verified by spectrophotometric scans at select sites across the pellicle aperture (all at 0° incidence). The objective in this test was to discern site-dependent wavelength peak shifts in the etalon spectral peaks in response to path-length differences. Again, within instrument resolution, only null results were obtained. As one would expect, such pellicles "ring" under all realistic mounting conditions—interferometry in *reflection* is a fruitless exercise, even if the sample film is mounted on a lapped frame that, by itself, is interferometrically flat.

System-Integration Considerations

From a systems-integration viewpoint, these perfluorinated films offer advantages but also a few drawbacks. Although highly elastic, the membranes are only a few microns thick and, accordingly, vulnerable to mechanical attack. Rapidly changing air-pressure differentials across the membranes, or directed air bursts typical of procedures for dust removal from optical surfaces, may cause membrane rupture. Another challenge is the still-limited clear-aperture size available commercially. The laser systems mentioned at the outset are designed for near-40-cm clear aperture: to date no perfluorinated pellicle measuring *40 cm in every direction* has been made. The largest pellicles available to this laboratory are 30 cm × 40 cm and 30 cm in diameter (circular).

Owing to the "drumhead" vibrations, pellicles are not suitable for image-quality, *reflective* applications. If the requirement, however, is simply one of getting photon energy into a certain direction, such as toward spatially integrating detectors or sensors, this drawback will be irrelevant.

Another challenge is posed by the *very low surface energy* of perfluorinated polymers (well-known "Teflon® effect"). There is not great latitude in choosing materials for multilayer designs, as poor wettability of perfluorinated surfaces makes uniform spin deposition of other materials nearly impossible.

Summary

The advantages of freestanding polymer film pellicles, apparent from the foregoing discussion, are rapid fabrication (spin on, lift off, mount on frame), robustness against 351-nm laser damage, photolytic stability, chemical inertness, amorphous structure, excellent transmitted-wavefront uniformity, and absence of birefringence. The best pellicles tested to date show UV damage thresholds up to five times higher than the frequency-conversion crystals (KDP) required for converting glass-laser output to the UV.

ACKNOWLEDGMENT

We thank our contacts at the three vendors for their prompt and enthusiastic support: Dr. K. Itoh, Shin-Etsu; Dr. C. B. Wang, MicroLithography, Inc.; and Joseph. S. Gordon, DuPont Photomasks. We also thank William Castle for help with interferometry and Jay Anzelotti for assistance in refractive-index calculations and field-distribution evaluation. Evaporated thin films were prepared under the direction of D. Smith. This work was supported by the U.S. Department of Energy Office of Inertial Confinement Fusion under Cooperative Agreement No. DE-FC03-92SF19460 and the University of Rochester. The support of DOE does not constitute an endorsement by DOE of the views expressed in this article.

REFERENCES

1. *Energy and Technology Review*, Lawrence Livermore National Laboratory, Livermore, CA, UCRL-52000-94-12, 1 (1994).

2. Many empirical as well as fundamental research results on laser damage can be found in the series of proceedings from the Annual Symposia on High-Power-Laser Materials (Boulder Conferences) published by the U.S. Government Printing Office as Special NBS Publications (until 1990) and by SPIE (after 1990).

3. T. Shirasaki *et al*., in *Photomask and X-Ray Mask Technology*, edited by H. Yoshihara (SPIE, Bellingham, WA, 1994), Vol. 2254, pp. 392–400.

4. Shin-Etsu Chemicals, New Functional Materials Department, Research Center, Annoka, Gunma, Japan; DuPont Photomasks, Inc., Danbury, CT 06810; MicroLithography, Inc., Sunnyvale, CA 94089.

5. L. M. Sverdlov, M. A. Kovner, and E. P. Krainov, *Vibrational Spectra of Polyatomic Molecules* (Wiley, New York, 1974), p. 397.

6. J. R. Throckmorton, J. Org. Chem. **34**, 3438 (1969).

7. E. N. Squire, U.S. Patent No. 4,948,851 (14 August 1990); U.S. Patent No. 4,973,142 (27 November 1990).

8. D. L. Duly, H. Windischmann, and W. D. Buckley, U.S. Patent No. 4,523,974 (18 June 1985).

9. Hamamatsu U1381R-01, Hamamatsu Photonic Systems, Bridgewater, NJ 08807-0910.

10. Tektronix 7250, Tektronix, Inc., Beaverton, OR 97077.

11. M. R. Kozlowski *et al*., in *Laser-Induced Damage in Optical Materials: 1990*, edited by H. E. Bennett *et al*. (SPIE, Bellingham, WA, 1991), Vol. 1441, pp. 269–282.

12. Zygo Mark IV-XP, Zygo Corporation, Middlefield, CT 06455-0448.

13. K. M. Dyumaev *et al*., Bull. Acad. Sci. USSR Phys. Ser. **53**, 194 (1989).

14. While this manuscript was completed, 248-nm test results (15 ns) on select samples became available, buttressing the results listed here: T. Lehecka, U.S. Naval Research Laboratory (private communication). Request further information at lehecka@nemesis.nrl.navy.mil.

15. Corning 7940, Corning, Inc., Technical Products Division, Corning, NY 14831.

16. DuPont Mylar®, DuPont Packaging and Industrial Polymers, D-5100, Wilmington, DE 19898.

17. DuPont AF-1600, DuPont Fluoroproducts, Wilmington, DE 19880-0702.

18. S. Papernov, A. Schmid, and F. Dahmani, "Laser Damage in Polymer Waveguides Driven Purely by a Nonlinear, Transverse-Scattering Process," to appear in *Optics Communications*.